

Fly Your Satellite!

Analysis Report (ARPT)

Thermal Analysis



UNIVERSITAT POLITÈCNICA
DE CATALUNYA
BARCELONATECH

NANOSAT LAB



FLY YOUR SATELLITE!

Contents

1	Introduction	9
1.1	The PoCat-Lektron mission	9
1.1.1	Mission statement	9
1.1.2	Mission Objectives	9
1.2	System Description	9
1.2.1	Communications (COMMS)	10
1.2.2	Electrical Power System (EPS) & Power Generation	10
1.2.3	On-Board Computer (OBC)	11
1.2.4	Attitude Determination and Control (ADCS)	11
1.2.5	K-Band (P/L)	11
1.2.6	L-Band (P/L)	11
1.3	Structure	11
2	Thermal-Design Requirements	14
2.1	Component Temperature Ranges	15
3	Thermal Margins and Design Temperatures	17
4	Worst Hot and Cold Case Definition	18
4.1	External Heating Environment	18
4.2	Satellite Internal Heat Dissipation and Attitude	19
4.3	Worst Hot and Cold Cases	20
5	Thermal Model Description	21
5.1	Geometrical Mathematical Model	21
5.1.1	General assumptions	21
5.1.2	Material Properties	21
5.1.3	Printed Circuit Boards Conductivity and Specific Heat	22
5.1.4	Introduction to the GMM	24
5.1.5	Killswitches	25
5.1.6	Bottom Board	26
5.1.7	Slider Board	26
5.1.8	Battery and Battery Support (Case)	27
5.1.9	Vertical Conenctors	29
5.1.10	Spacers	29
5.1.11	Magnetorquer +Y	30
5.1.12	Attitude and Obrbit Determination and Control	31
5.1.13	Electrical Power Supply	32
5.1.14	On Board Computer and Communications	33
5.1.15	Payload (K-Band)	34
5.1.16	Lateral Boards and Solar Panels	36
5.1.17	COMMS Antenna	38
5.2	NGTNs and User Defined Conductors	39
5.2.1	Non-Geometrical Thermal Nodes	39
5.2.2	Spacers	39
5.2.3	Antenna	40

Acronyms

BOL Begin of Life

CAD Computer Aided Design

EOL End of Life

ETSETB Barcelona School of Telecommunications Engineering

EU European Union

FEM Finite Element Model

GMM Geometrical Mathematical Model

ICD Interface Control Document

IR Infrared

NOTR Non-Operational Temperature Ranges

OTR Operational Temperature Ranges

PCB Printed Circuit Board

TBD To be determined/defined

TCS Thermal Control System

TMM Thermal Mathematical Model

TRP Temperature Reference Point

VCD Verification Control Document

List of Figures

1.1	Physical architecture of ^{Po} Cat 3 block diagram.	10
1.2	The ^{Po} Cat 1,2,3 PocketQubes as of 2024.	11
1.3	PocketQube reference frame.	12
1.4	Basic Structure of the ^{Po} Cat spacecraft.	12
1.5	Colored K-Band PQ Structure	13
3.1	Temperature Margins Definitions for the TCS	17
5.1	Example or IR emissivity calculation on simplification of pieces	22
5.2	Simplification of PCB layers	22
5.3	Exploded view of the ^{Po} Cat-3 spacecraft.	24
5.4	Full GMM in ESATAN and in Solidworks.	24
5.5	PocketQube GMM in ESATAN and Solidworks w/o a lateral board.	25
5.6	Comparison between thermal and CAD model for the Killswitches (with other components).	25
5.7	Comparison between thermal and CAD model for the Killswitches (wtohut other components)	25
5.8	Comparison between thermal and CAD model for the Bottom Board.	26
5.9	Comparison between thermal and CAD model for the Slider Board (with other components)	27
5.10	Comparison between thermal and CAD model for the Slider Board (without other components)	27
5.11	Comparison between thermal and CAD model for the Battery Support (with battery)	28
5.12	Comparison between thermal and CAD model for the Battery Support (without battery)	28
5.13	Comparison between thermal and CAD model of the vertical connectors.	29
5.14	Comparison of spacers in ESATAN and in Solidworks.	30
5.15	Comparison between thermal and CAD model for the MTG +Y (Top View)	31
5.16	Comparison between thermal and CAD model for the MTG +Y (Isolated View)	31
5.17	Comparison between thermal and CAD model for the AOCS (Top View)	32
5.18	Comparison between thermal and CAD model for the AOCS (Bottom View).	32
5.19	Comparison between thermal and CAD model for the EPS (Top View)	33
5.20	Comparison between thermal and CAD model for the EPS (Bottom View).	33
5.21	Comparison between thermal and CAD model for the OBC and COMMS Model (Top View)	34
5.22	Comparison between thermal and CAD model for the OBC and COMMS Model (Bottom View)	34
5.23	Comparison between thermal and CAD model for the K-Band Payload.	35
5.24	Comparison between thermal and CAD model for the K-Band Payload without support,	35
5.25	Comparison between thermal and CAD model for the K-Band Payload support.	35
5.26	Comparison between thermal and CAD model for the K-Band Payload support (bottom view).	35
5.27	Comparison between thermal and CAD model for the lateral boards.	37
5.28	Comparison between thermal and CAD model of an empty PQ.	37
5.29	Comparison between thermal model and image of the COMMS Antenna.	38
5.30	Spacers with GLs between them in ESATAN.	40
5.31	Antenna connected to a lateral board through a UDC in ESATAN.	40

List of Tables

2.1	NOTR and OTR of the most relevant components	15
2.2	Operational Temperature Limits by Subsystem.	16
3.1	Acceptance and design temperature ranges for subsystems and components.	17
4.1	External heating environment orbit parameters.	18
4.2	Design hot and cold external heating environments	18
4.3	Satellite operating modes, mean power consumption and attitude states.	19
4.4	Worst Hot and Cold Cases.	20
5.1	Material Properties Table. *LiPo Battery values are approximated.	21
5.2	Cumulative thickness of material layers by PCB	23
5.3	PCB Bulk Thermal Properties	24
5.4	Bulk properties of the killswitches.	26
5.5	Optical properties of the killswitches primitives.	26
5.6	Bulk properties of the bottom PCB.	26
5.7	Optical properties of the bottom board primitive.	26
5.8	Slider board primitives bulk properties. Mass percentage is calculated by volume and density.	27
5.9	Optical properties of the slider board primitives.	27
5.10	Bulk properties of the battery.	28
5.11	Battery support primitives bulk properties.*Adjusted density to ESATAN volume.**Considering the screw inside.	28
5.12	Optical properties of the LiPo Battery.	29
5.13	Optical properties of the battery support.	29
5.14	Bulk properties of the vertical connectors primitives.	29
5.15	Optical properties of the vertical connectors.	29
5.16	Bulk properties of the spacers primitives.	30
5.17	Optical properties of the spacers.	30
5.18	Bulk properties of the magnetorquer (Positive Y axis) primitive.	31
5.19	Optical properties of the MTQ+Y.	31
5.20	Bulk properties of the AOCS board.	32
5.21	Optical properties of the AOCS PCB primitive.	32
5.22	Bulk properties of the EPS board primitive.	33
5.23	Optical properties of the EPS PCB primitive.	33
5.24	Bulk properties of the OBC-COMMS PCB primitive.	34
5.25	Optical properties of the OBCCOMMS PCB primitive.	34
5.26	Bulk properties of the P/L Under PCB.	36
5.27	Bulk properties of the P/L Top (+Antenna) PCB. The antenna properties are assumed to be the same as for the PCB (approximation).	36
5.28	Bulk properties of the K-Band Support.	36
5.29	Optical properties of the K-Band payload.	36
5.30	Bulk properties of the lateral boards.	37
5.31	Bulk properties of the solar panels.	37
5.32	Optical properties of the lateral boards and the solar panels.	38
5.33	Bulk properties of the COMMS Antenna.	38
5.34	Optical properties of the COMMS antenna.	38
5.35	NGTNs UDC assigned values.	39

APPROVAL

Title FYS DRD and Guidelines			
Issue Number	1	Revision Number	0
Author		Date	
Approved By		Date of Approval	

CHANGE LOG

Reason for change	Issue Nr	Revision Number	Date
First release	1	0	
Second release	2	0	

CHANGE RECORD

Issue Number	Revision Number		
Issue Number	1	Revision Number	0
Reason for change	Date	Pages	Paragraph(s)
First release			
Second release			

DISTRIBUTION

Disclaimer

This document has been prepared for use by the Fly Your Satellite! PoCat Lektron team.

**This document shall be considered confidential and not to be distributed further without permission of
ESA Education, and the authors.**

Applicable Documents

Reference	Document Title	Issue/Release Date
RD01	ECSS-E-ST-31C Space Engineering	Issue 2, 2008/11/15
RD02	ECSS-E-HB-31-01 - Space Engineering - Thermal design handbook - Part 1 to 16	multiple
RD03	P. D.G. Gilmore, "Spacecraft Thermal Control Handbook: Fundamental Technologies", ESA-TEC-MTT	2002

1 Introduction

The ^{Po}Cat-Lektron Thermal Analysis is aimed to verify that all the components of the spacecraft work in its operational temperature range during all mission phases. In order to develop an accurate enough model, the following approach has been considered:

First, an isothermal solid cube will serve as an initial model. After that, models considering radiation as the principal mode of heat transfer will provide more accurate results. Later on, models considering both conduction and radiation as the main modes of heat transfer will allow the needed characterization of the spacecraft to verify the thermal requirements of each component.

In this document, the isothermal analysis and the radiation analysis of the ^{Po}Cat 2 and ^{Po}Cat3 satellites are presented.

The main objective of the isothermal analyses is to identify a passive thermal control which maintains the spacecraft temperature in the correct behavior. In this case, the evaluated technique is the use of different paints on the spacecraft surface.

As for the radiation analyses, they are aimed to validate the spacecraft thermal model and verify its behavior under different heating environments.

1.1 The ^{Po}Cat-Lektron mission

1.1.1 Mission statement

The ^{Po}Cat-Lektron is a mission resulting from the IEEE OpenPocketQube Kit initiative, developed at the UPC NanoSat Lab. The mission has been selected in the 4th call of the ESA Fly Your Satellite! (FYS) program. The mission analysis presented corresponds to the ^{Po}Cat-Lektron mission. It consists of two 1P PocketQubes, the PoCat-2 and the PoCat-3, developed as a part of the IEEE OpenPocketQube Kit. This mission aims to demonstrate the feasibility of PocketQube platforms for remote sensing applications.[1]

The payloads on board of the PocketQubes are two passive radiometers to be used for RFI purposes on K and L bands. Apart from the remote sensing nature of the mission, this mission also aims to demonstrate the feasibility of the PocketQube platforms to create, manage and join Federated Satellite Systems. To do so, the FSS Experiment will be reproduced as a part of the experiments of the mission.

1.1.2 Mission Objectives

- **Demonstration of Scientific Viability:** Demonstrate the feasibility of conducting scientific missions using PocketQube platforms. To do so, the mission proposes collecting valuable RFI data through a K-Band and L-Band passive radiometers (One for each PocketQube). The payloads will monitor interferences on these bands. This data will facilitate enhanced detection and the generation of heatmaps indicating RFI distribution across the globe. In this experiment we aim to obtain data on the K-Band to see the impact on the atmospheric water vapor measurements, and in the L-Band the interferences over the Position Navigation and Timing (PNT) signals.
- **Satellite Federation Concept:** To establish and demonstrate that PocketQube platforms can create, manage and join Federated Satellite System (FSS). This proof of concept for this resource-limited platforms is based on the reproduction of the FSS Experiment conducted at the UPC NanoSat Lab. The demonstration consists on creating a federation between 2 PocketQubes, in order to download data. Previous missions such as the FSS-Cat from the UPC NanoSat Lab demonstrated the feasibility of this opportunistic collaboration using 6U CubSats.
- **Educational Development:** As a mission developed at the UPC NanoSat Lab, the mission is oriented for undergraduate students to gain experience and get involved in real space missions. In addition, several Bachelor and Master Thesis had been done from this project, apart from the academic papers that this project has produced.

1.2 System Description

The physical architecture of the spacecraft (S/C) is comprised by the different subsystems and components, as well as the electrical lines that provide communication between them. A PocketQube architecture is relatively simple

compared to bigger spacecrafts, even when compared to CubeSats. The system straightforwardness is given by the use of an individual Microcontroller Unit (MCU). This approach, while necessary due to power and space (size) constraints, centralizes the S/C, and, while it creates a single point of failure, it also minimizes complexity.

A block diagram of the spacecraft (^{Po}Cat 3) physical architecture is provided up next:

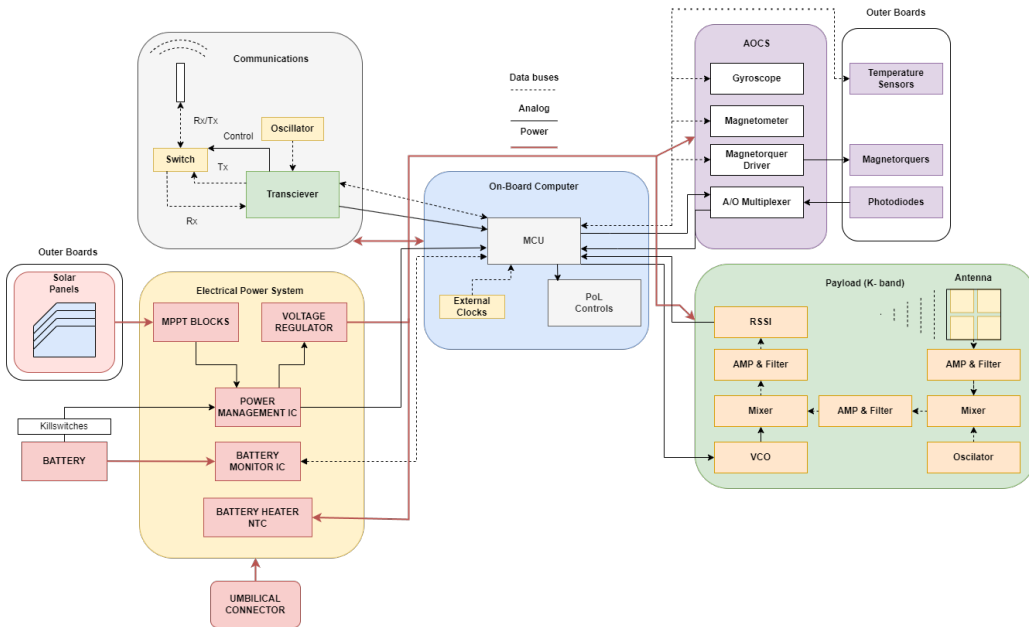


Figure 1.1: Physical architecture of ^{Po}Cat 3 block diagram.

1.2.1 Communications (COMMS)

The COMMS subsystem main fuctions are to receive and send data through radio frequency (RF) waves. To do so it is provided of a monopole quarter-wavelenght antenna, with an approximate lenght of 8.6cm, designed to transmit at 868MHz. The signals to be sent by the spacecraft (telemetry) are generated and modulated by the transciever (combination of a radio transmitter and receiver). The signals received are also demodulated at the transciever.

The system is half-duplex as radio information (transmission and reception) can not be Tx'd and Rx'd at the same time. This is due to both the transciever capabilities and the use of a switch. The later regulates wether information is to be received or transmitted, and is controlled by the transciever itself which is, at the same time, controlled bu the MCU. In fact, all transciever control is done by the MCU through a Serial Peripheral Interface (SPI).

1.2.2 Electrical Power System (EPS) & Power Generation

The EPS subsystem manages power distribution and regulation. Energy is obtained into the system through solar panels located at the lateral boards of the PocketQube. This energy is regulated by the MPPT blocks, one for each panel, and subministrated to the battery. Note that the killswitches ensure the satelite can't turn on when in it's rail before being deployed.

Power is distributed to the rest of the system after passing through the voltage regulator. A battery heater is located in this board. The heater ensures that the battery temperature is constrained to higher than it's lowest operating temperature and will be an object of interest in this report.

Finally, power can also be provided through the umbilical connector, still passing through the killswitches. The umbilical connector also allows code flashing into the MCU.

1.2.3 On-Board Computer (OBC)

The OBC subsystem's main component is the microcontroller unit (MCU). The MCU is in control of all data handling and on-board processing, acting as the brain of the spacecraft. Almost all information goes to or comes from the MCU and it is all stored there, either in its flash memory or in its random access memory (RAM).

Physically, on the OBC board will also be located the COMMS subsystem as well as point of load (PoL) controls and external clocks to ensure the proper timing of the MCU.

1.2.4 Attitude Determination and Control (ADCS)

The ADCS subsystem is the responsible for, as the name indicates, attitude determination and control. To do so it is equipped with a gyroscope, to measure its angular velocity, a magnetometer to measure the local magnetic field, the magnetorquer driver, which controls the intensity that circulates through the magnetorquers, square, plain coils located at the lateral boards that provide torque via electromagnetic interactions, as well as an A/O Multiplexer that provides information on sun position.

Temperature sensors are also placed on the lateral boards in order to provide insight for future missions, as a tumbling mode to avoid heat is not possible with the current architecture.

1.2.5 K-Band (P/L)

The payload on ^{Po}Cat 3 measures RFI interference on the K-Band. To do so it is equipped with a patch antenna, several amplifiers and filters as well as mixers, one regulated by an oscillator and the other by a voltage controlled oscillator (VCO).

1.2.6 L-Band (P/L)

The payload on ^{Po}Cat 2 measures RFI interference on the L-Band. The main difference between both payloads is the antenna used, being in this case a helicoidal deployable antenna.



Figure 1.2: The ^{Po}Cat 1,2,3 PocketQubes as of 2024.

1.3 Structure

This project follows the PocketQube mechanical standard. The satellite then, according to the 1P standard, consists of a $50 \times 50 \times 50 \text{ mm}^3$ cube, placed onto a $64 \times 58 \text{ mm}^2$ interface board, the latter acting as the mechanical interface between the satellite and the deployer pod. The contact is done by having PCB edges represented in grey in the figure below slide into the deployer rails, with the cube being fixed and later launched along the +Z direction. This interface board serves only the purpose described above. In the -Y direction, another PCB is mounted in order to house the circuitry correspondent to the ventral side of the cube.

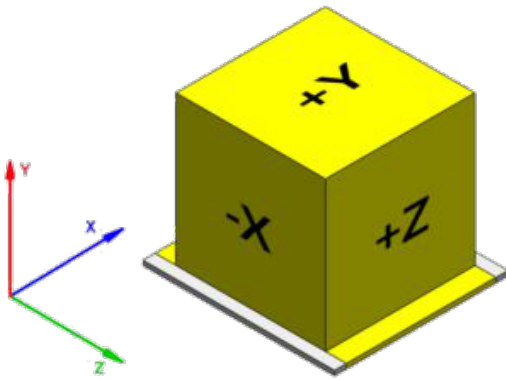


Figure 1.3: PocketQube reference frame.

The proposed solution for the inner structure is presented below:

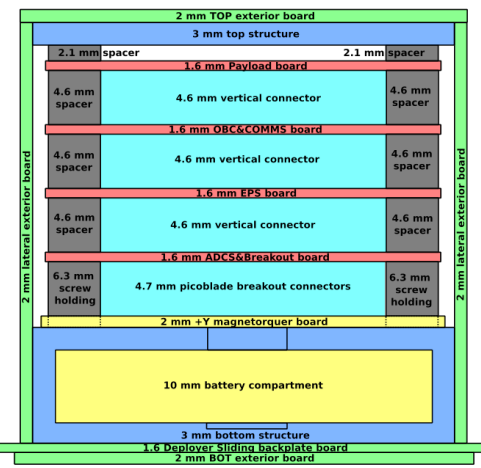


Figure 1.4: Basic Structure of the^{Po}Cat spacecraft.

In **green**, we can see the outer boards, which form the external part of the satellite. On the bottom exterior board, the killswitches are located, while the deployer sliding backplate will be the only PCB in contact with the deployer rail. Consider that the top exterior board is subject to the payload used for each satellite. If the payload can be implemented on a single PCB (Payload board), this top exterior board remains in place. In the case of our payloads, both the K-Band and the L-Band, the top exterior board is replaced by the payload board.

In **blue**, we can see the only two internal structures that are not PCBs. The bottom structure will house the battery and act as an interface between the bottom exterior board and the sliding plate, connecting them with the rest of the subsystem stack. This structure will be made of PTFE (Teflon). The top structure, made of 7075 Aluminium Alloy, will be used for the K-Band, acting as the interface between the payload and the rest of the subsystem stack. Additionally, both structures will allow the lateral boards to be screwed into them.

In **red**, we find the PCBs that form the various subsystems. From top to bottom, these are: the Payload board (for the payload, additional PCBs may be added inside the payload), the OBC and COMMS board, the EPS board, and the ADCS board. These PCBs are connected to each other via the vertical connectors, shown in **cyan**, which allow electrical interconnection between all the PCBs in the stack.

In **gray**, spacers distribute the force from the tightened screws, preventing the vertical pins from bearing the full load.

Finally, in **yellow**, see the +Y magnetorquer and the battery.

More information on the materials is provided in its corresponding section. The K-Band PQ structure:



Figure 1.5: Colored K-Band PQ Structure

2 Thermal-Design Requirements

The Thermal Control System (TCS) requirements for ^{Po}Cat 2/3 S/C affecting the thermal design are listed below:

- **TCS-001**

The TCS shall ensure that each hardware component works in its operational temperature range during all mission phases (until the end of the operating lifetime).

- **TCS-002**

The TCS shall control the spacecraft temperature using passive and active mechanisms.

- **TCS-003**

The TCS should be designed in accordance with "Space engineering: Thermal control general requirements" [RD01].

- **TCS-004**

The satellite acceptance margin shall be 5°C.

- **TCS-005**

The TCS design shall be conceived using Earth and sun the natural environment specified in [RD01].

- **TCS-006**

The OBC shall provide the satellite housekeeping data to the TCS in order to monitor and control the satellite temperature.

- **TCS-007**

The TCS design shall make use of materials and design features compatible with the environmental factors expected during all mission phases including possible effects and degradations.

- **TSC-008**

The satellite qualification margin shall be 5°C.

- **TSC-009**

An uncertainty margin of 10°C shall be applied to predicted temperatures.

The objective then, of this document, will be to provide, as accurately as possible, information in regards to the fulfilling of the aforementioned requirements. Do acknowledge that the results presented do not, by themselves, verify the requirements and call for the need of experimental procedures (TVAC Testing).

2.1 Component Temperature Ranges

In order to help define and verify requirements related to the temperature of individual components, and the full system, the information provided in the datasheets of each component is compiled and presented in this subsection.

The Non-Operational Temperature Ranges, constituting the temperatures where the part is safe to be stored, and the Operational Temperature Ranges, constituting the temperatures indicated by the manufacturer of guaranteed performance, of all satellite subsystems most important components are shown in Table 2.1:

Components	Non-Operational Temperature Range		Operational Temperature Range	
	Min	Max	Min	Max
ADCS				
LPV542	-65	150	-40	125
IIM-42652	-40	125	-40	105
MMC5983MA	-55	125	-40	105
TMUX1108	-65	150	-40	125
BD2606MVV	-55	150	-30	85
Lateral boards				
TCN75AOA	-65	150	-40	125
Photodiodes	-40	125	-40	125
EPS				
SPV1040	-40	150	-40	125
LTC4040	-65	125	-40	125
DS2782	-55	125	-40	85
ISL9120IR	-65	150	-40	85
SIR424DP	-55	150	-55	150
OBC & COMMS				
STM32L476	-65	150	-40	85
BD2232G	-55	150	-40	85
BGS12PL6E6327XTSA1	-55	150	-40	85
FA-128_32.0000MF20X-K5	-40	125	-40	85
ABS09-32.768KHZ-7-T	-55	125	-40	85
ECS-120-18-33-JEM-TR3	-55	125	-20	70
SX1262 RX & TX	-55	125	-55	125
Payload K - Band				
HMC342	-65	150	-55	85
BFHK-2582+	-55	125	-55	125
HMC260	-65	150	-55	85
HMC506LP4	-65	150	-40	85
CY2-44+	-65	150	-40	85
HMC516LC5	-65	150	-40	85
HFCN-5500+	-55	100	-55	100
CMD271P3	-55	150	-40	85
LFCW-8000+	-55	125	-55	125
SIM-14+	-55	100	-40	85
HMC358MS8G	-65	150	-40	85
LEE2-6+	-65	150	-40	85
B39871B4316P810	-40	85	-40	85
LT5537	-65	125	-40	85
LT3048IDC-TRMPBF	-65	150	-40	125
MIC2215-AAAYML-TR	-65	150	-40	125
AD8224ACPZ-R7	-65	130	-40	125

Table 2.1: NOTR and OTR of the most relevant components

In Table 2.2 the OTR are grouped by subsystem, extracting from Table 2.1 the most limiting temperatures of the used components used, as all subsystems are in-house developed. Note that these are not the Design Temperature Ranges.

In Section 3 the applied Qualification and Acceptance Thermal Margins are described and the Acceptance and Design Temperature Ranges are provided.

Subsystem	Operational Temperature Range(°C)	
	Min	Max
EPS	-40	85
AOCS	-30	85
OBC/COMMS	-20	70
K-Band	-40	85
L-Band	-40	85
Top Board	-40	125
Lateral Boards	-40	125
Bottom Board	-40	85
Battery (Charge)	0	45
Battery (Discharge)	-20	60

Table 2.2: Operational Temperature Limits by Subsystem.

Note that the OTR of the battery is also provided in the table due to the criticality of its correct operation and its restrictive temperature ranges.

3 Thermal Margins and Design Temperatures

In order to account thermal-model inaccuracies, unpredictable TCS-related events and any other unexpected events, the following thermal margins have been applied to all satellite components and the calculated temperatures as defined in [RD02]:

Thermal Uncertainty Margin

The Thermal Uncertainty Margin is a margin of safety applied to all calculated temperatures in order to account for inaccurate physical, environmental and modeling parameters. A $\pm 10^{\circ}\text{C}$ uncertainty margin has been taken in this analysis.

Acceptance Thermal Margin

The Acceptance Thermal Margin is a contingency to account for unpredictable TCS related events. A $\pm 5^{\circ}\text{C}$ acceptance margin for all the components has been considered in this analysis.

Qualification Thermal Margin

The Qualification Thermal Margin is a contingency to account for unexpected events. A $\pm 5^{\circ}\text{C}$ qualification margin for all the components has been considered in this analysis.

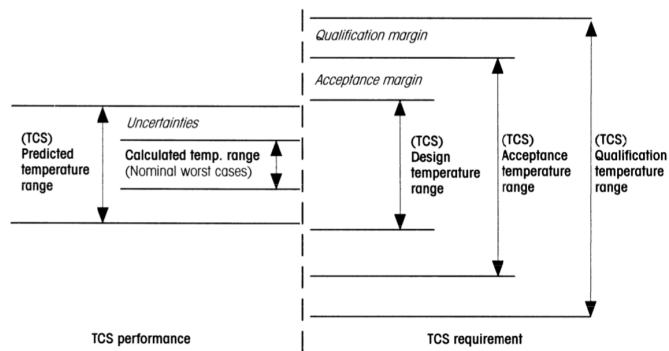


Figure 3.1: Temperature Margins Definitions for the TCS

After the application of the above margins to the Operational Temperature Ranges (2.2) as shown in 3.1, the Acceptance and Design Temperature Ranges are shown in Table 3.1.

Subsystem/Component	Acceptance Temperature Range ($^{\circ}\text{C}$)		Design Temperature Range ($^{\circ}\text{C}$)	
	Min	Max	Min	Max
EPS	-35	80	-30	75
AOCS	-25	80	-20	75
OBC/COMMS	-15	65	-10	60
K-Band	-35	80	-30	75
L-Band	-35	80	-30	75
Top Board	-35	120	-30	115
Lateral Boards	-35	120	-30	115
Bottom Board	-35	80	-30	75
Battery (Charge)	5	40	10	35
Battery (Discharge)	-15	55	-10	50

Table 3.1: Acceptance and design temperature ranges for subsystems and components.

The predicted temperature ranges, i.e. the temperature ranges obtained by analyses (calculated temperature range), adjusted by the thermal uncertainty margin, must be within the Design Temperature Range under all circumstances.

4 Worst Hot and Cold Case Definition

4.1 External Heating Environment

P^o Cat-2 and P^o Cat-3 are expected to be launched together, from a yet to define launcher. They will perform, ideally, a polar or quasipolar orbit with near-zero eccentricity. In table 4.1 the most critical external heating environment orbit parameters taken in the analyses present in this document (unless otherwise specified).

Do note that as of the latest revision of this document the selected launcher and final orbit parameters are still an unknown matter. Therefore, within reasonable bounds, the calculations will be presented considering the extremal ranges of these boundary conditions.

Parameter	Value
Perigee height	450–500 km
Eccentricity (e)	0
Inclination (i)	80–100
Estimated launch date	2026–Q2

Table 4.1: External heating environment orbit parameters.

Extreme hot and cold heating environments have been defined in order to envelop all possible cases in between. Table 4.2 summarizes the design hot and cold environments where extreme and less pessimistic values suggested in RD03 (2σ) have been taken respectively. In this table, the **solar flux** maximum and minimum taken values have been those corresponding to the winter and summer solstices respectively as specified in RD03.

Regarding the **Earth albedo** and the **Earth Infrared**, values from RD03 have been taken, using a 2σ margin. The time period taken is of 90 minutes, which approximately coincides with orbit time, neglecting variations on lower time scales. The appropriate non-Lambertian corrections have been applied as specified in the reference document.

The **duration of the eclipses** can also have a high impact on the maximum and minimum temperatures reached by the satellite during an orbit. The most extreme cases (i.e., the shortest and longest eclipse times) have been considered for the orbit inclination shown in Table 3. To this aim, the so-called **orbit beta angle** β has been defined for each case as the minimum angle between the orbit plane and the solar vector. For the cold case, the beta angle is 0° since the longest eclipse occurs when the orbit plane is parallel to the Ecliptic. As for the hot case, the shortest eclipse occurs when the value of β is closest to $\pm 90^\circ$. Since the Earth axial tilt (ϵ_E) is 23.44° , the maximum beta angle can be obtained as the sum of the Earth tilt angle and the spacecraft orbit inclination as:

$$\beta_{\max} = \epsilon_E + i \quad (1)$$

Despite this, due to the inclination being yet unknown, the most extreme values are taken.

Heating Environment	Solar Irradiance (W/m^2)	Earth Albedo	Earth IR (W/m^2)	β ($^\circ$)
Hot Case	1414	0.55	219	90
Cold Case	1322	0.22	238	0
Extreme Hot Case	1414	0.8	261	90
Extreme Cold Case	1322	0.05	189	0

Table 4.2: Design hot and cold external heating environments

It needs to be noted that the later values presented in Table 4.2 represent extreme (eventually non-physically possible) situations aiming to envelop the hottest and the coldest possible heating environments the spacecraft will encounter. The non-extreme parameters of the table will be the ones used to perform the thermal analysis of the spacecraft.

4.2 Satellite Internal Heat Dissipation and Attitude

The satellite operating modes defined, from the internal heat dissipation point of view, are the following:

- **Standby (Sb)**: Period before the satellite is turned on. All subsystems are inactive.
- **Released (R)**: After the standby period, the satellite is turned on, with the EPS and OBC as the only active subsystems.
- **Pre-detumbling (PD)**: Once the COMMS antenna has been deployed, the EPS, OBC, COMMS and AOCS (only determination for telemetry) are active. The COMMS subsystem is transmitting data with a ratio of 1% of the orbit time.
- **Detumbling (D)**: Same as pre-detumbling state, with the magnetorquers operating.
- **Detumbled (Dd)**: Once the satellite is detumbled, the AOCS is keeping the desired attitude. The COMMS subsystem is transmitting data with a ratio of 1% of the orbit time.
- **Nominal (N)**: Satellite is fully operative. The payload is executed a yet to define number of times per orbit. The COMMS subsystem is transmitting data with a ratio of 1% of the orbit time.
- **Contingency (C)**: When the batteries fall below a certain value. In this mode, some functionalities of the flight software are disabled (P/L, Nadir, FSS).
- **Survival (S)**: After an unexpected anomaly in battery levels, the satellite enters this mode. Transmissions are ceased.
- **Satellite Off (OFF)**: Satellite turned off during its operation due to unexpected events. All subsystems are inactive.

As for the satellite attitude, the following states have been considered:

- **Nadir Pointing (NP)**: Satellite -Z face pointing towards Earth center. Desired (ideal) attitude of the spacecraft achieved by the AOCS during its operation.
- **Random Rotation (RR)**: Satellite randomly rotating about its three axes (e.g., during the deployment).
- **Zenith Pointing (ZP)**: Satellite +Z face pointing towards Earth center (-Z face pointing towards zenith). Critical situation considered, as a worst-case assumption.

The mean power consumption of each satellite operating mode, and the satellite attitude state in which they can occur, are summarized in Table 4.3. Mean power consumption values have been extracted from the power budget yet to be presented.

Operating Mode	Power Consumption (mW)	Attitude State	COMMS Config.
Commissioning Phase			
Standby (Sb)	0	RR	Stowed
Released (R)	74	RR	Stowed
Pre-detumbling (PD)	497	RR	Deployed
Detumbling (D)	995	RR	Deployed
Detumbled (Dd)	497	NP	Deployed
Operational Phase			
Nominal (N)	497	NP	Deployed
Contingency (C)	77	NP	Deployed
Survival (S)	46	NP	Deployed
Satellite Off (OFF)	0	NP	Deployed

Table 4.3: Satellite operating modes, mean power consumption and attitude states.

Do note that, after the release, the spacecraft will enter an initial (Init) state (Released) where it'll begin the deployment process of the COMMS antenna, only entering the Nominal mode after communication has been established with the Ground Station.

In this thermal analysis only worst hot and cold cases have been studied, enveloping all possible cases in between. From a thermal point of view, the RR attitude state is less critical than the NP and ZP states; since the satellite is constantly rotating, the heat flux is expected to be averaged between the different faces. Finally, it is not clear whether the deployed or the stowed configuration corresponds to the worst hot and cold case. Despite this, due to the limited size of the COMMS Antenna, it is expected to find a non significative difference, and, therefore, this analysis will only evaluate the deployed case.

From the satellite modes during the operational phase, only Nominal and Survival modes will be analyzed, since these are the modes with the higher and lower power consumption respectively. It is expected that the Survival mode will be of most criticality due to the shutting off of the battery heater, in favour of a lower power consumption.

From the attitude point of view, the NP state will be analyzed. The ZP state might be considered in future analysis if required. This is due to the fact that this mode is not expected to present a relevant probability of occurrence.

4.3 Worst Hot and Cold Cases

Having defined the hot and cold heating environments and the hot and cold satellite internal heat dissipation and attitude cases, the overall worst cases are summarized in Table 4.4.

Operating Mode	Attitude State	COMMS Config.	Heating Environment
Prior to Detumbling			
Worst Hot Case	D	RR	Deployed
Worst Cold Case	Sb	RR	Deployed
Operational			
Worst Hot Case	N	NP	Deployed
Worst Cold Case	SS	NP	Deployed

Table 4.4: Worst Hot and Cold Cases.

5 Thermal Model Description

In this chapter the Geometrical Mathematical Model (GMM) and the Thermal Mathematical Model (TMM) will be discussed and presented, in respective order. Both models have been created and evaluated with the use of **ESATAN-TMS 2022** (Project Revision 1.445).

5.1 Geometrical Mathematical Model

The following section is composed, firstly, by the establishment of general assumptions, followed by a description of material properties, and, finally, by a detailed explanation of every modelled piece and subsystem.

5.1.1 General assumptions

The following general assumptions have been taken in the created models and performed simulations:

- External thermal sources and environment have been considered as presented in Section 4.
- The initial spacecraft temperature is 25°C .
- The satellite y-axis (+Y face) is always pointing to Nadir.
- Black paint is used in the internal PCBs of the satellite.
- White paint is used in the lateral and bottom PCBs.
- All PCBs can be modeled as a parallel (in-plane) and serial (cross-plane) set of thermal resistances defined by the properties of the materials they are constituted of.
- Electrical components can be modeled as Non-Geometrical Thermal Nodes with a set conductance and heat dissipation.
- All thermal and optical properties are not functions of temperature.

Despite this, some other approximations are taken in order to heavily simplify the geometry of certain pieces, most notably, the K-Band support and the threaded screws. Both will be discussed in further sections.

5.1.2 Material Properties

This subsection presents the different optical and thermal properties of the materials that have been used to define the bulks of the thermal model of the spacecraft. Seldom are these values directly assigned to a geometry, using instead more complex combinations of them, coupled with the use of the measured mass of components.

Material	ε_{IR}	α_s	ρ [kg/m ³]	c_p [J/kg·K]	k [W/m·K]
FR-4	0.94	0.12	1850	1200	0.8181
Copper	x	x	8930	385	400
Teflon (PTFE)	0.92	0.046	2070	1010	0.27
Stainless Steel (AISI304SS)	0.075	0.42	8000	500	15
Aluminum Alloy (Alloy 7075)	0.21	0.18	2810	960	130
RS Rogers	x	x	2200	960	0.2
Tin	0.11	0.08	5765	250	62
LiPo Battery*	0.3	0.5	2750	1000	2.5 (ip), 0.6 (cp)
Phosphor Bronze	x	x	8800	380	62
Aluminum 6063-T5	0.77	0.8	2700	900	209
Nylon	0.85	0.12	1150	1500	0.53
Gallium Arsenide	0.85	0.91	5316	325	50
ABS	0.82	0.94	1070	1990	0.162
White Paint	0.94	0.19	x	x	x
Black Coat	0.94	0.96	x	x	x

Table 5.1: Material Properties Table. *LiPo Battery values are approximated.

In order to determine the properties that are assigned to ESATAN primitives the following procedure is followed:

- **IR emissivity (ε_{IR}):** The IR emissivity is computed by performing a weighted average, by projected surface, of the conjunction of pieces modeled.

$$\varepsilon_{IR} = \sum_i \frac{A_i \cdot \varepsilon_i}{A_T} \quad (2)$$

Where A_T denotes the sum of all projected areas. An illustration of this process is provided below:

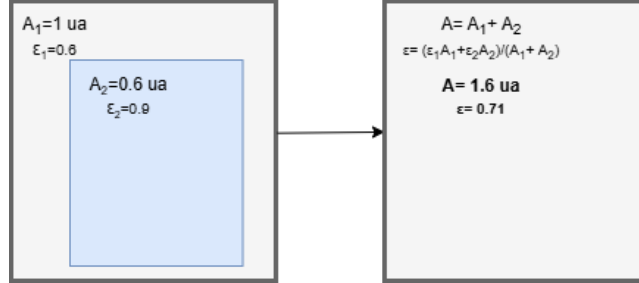


Figure 5.1: Example of IR emissivity calculation on simplification of pieces

- **Solar Absorptivity (α_s):** Solar Absorptivity is calculated following the same procedure as for the IR emissivity:

$$\alpha_s = \sum_i \frac{A_i \cdot \alpha_i}{A_T} \quad (3)$$

- **Density(ρ):** The density is computed by dividing the mass of the real component or components by the volume of the ESATAN primitive defined.

$$\rho = \frac{m_{real}}{V_{primitive}} \quad (4)$$

- **Specific Heat (c_p):** The specific heat is computed as the weighted sum of the individual specific heats by mass of each real component:

$$c_p = \sum_i \frac{c_i \cdot m_i}{m_T} \quad (5)$$

Where m_T denotes the sum of all masses.

- **Conductivity(k):** The conductivity calculations will be further discussed in the corresponding sections of each geometry as well as in the next subsection. The approach taken is to consider different pieces as series or parallel resistances, computing either the weighted averaged or the harmonic mean. This will lead to the appearance of in-plane and crossplane conductivities, denoted as i.p. or c.p. respectively.

5.1.3 Printed Circuit Boards Conductivity and Specific Heat

The PoCat space crafts make use of PCBs for the lateral boards as well as for the housing of the subsystems. Each one possesses a different amount of layers and even materials, leading to variations in conductivity. In order to simplify this problem each layer is considered a resistance, ignoring the order of placement.

This can be visually represented as:

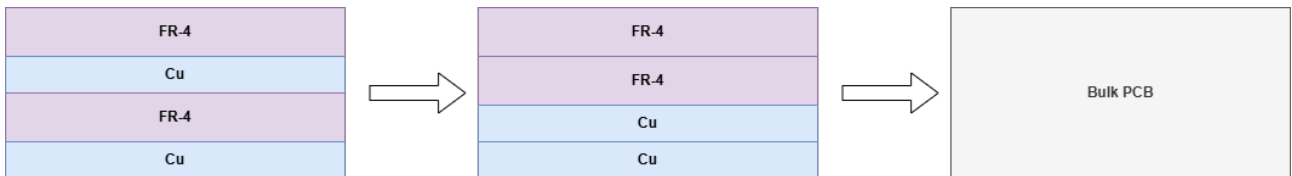


Figure 5.2: Simplification of PCB layers

Considering the amount of layers and the cumulative thickness of each type we arrive to the following table, containing information of each one of the PCBs. Note that the antenna P/L board is also computed.

PCB	Copper (mm)	FR4 (mm)	Mask (mm)	Rogers (mm)
OBC-COMMS	0.14	1.44	0.02	0
EPS	0.14	1.44	0.02	0
ADCS	0.14	1.44	0.02	0
Y+Mag	0.21	1.77	0.02	0
Laterals	0.21	1.77	0.02	0
Bottom	0.21	1.77	0.02	0
Slider	0.07	1.51	0.02	0
Kband Under	0.21	0.84	0.04	0.21
Kband Over (Antenna)	0.14	1.12	0.04	0.254

Table 5.2: Cumulative thickness of material layers by PCB

Now, in order to compute the c_p as well as i.p. and c.p. conductivities we will proceed with the aforementioned methods. To calculate the conductivities we will make use of the following formulas, corresponding to the weighted and harmonic means, respectively.

The in-plane conductivity:

$$\kappa_{i.p.} = \sum_i \frac{\kappa_i \cdot l_i}{l_T} \quad (6)$$

Where κ_i denotes the in-plane conductivity of each material, l_i its thickness and l_T the total thickness of the PCB.

The cross-plane conductivity:

$$\kappa_{c.p.} = \left(\sum_i \frac{l_i}{\kappa_i} \right)^{-1} \cdot l_T \quad (7)$$

Finally, the specific heat (c_p) can be computed, by imagining the PCB as an homogeneous substance, making use of the weighted average by mass of each layer. This yields the following expression:

$$c_p = \sum_i \frac{m_i \cdot c_p^i}{m_T} \quad (8)$$

Due to the impossibility of measuring each layers' mass we can make use of its relation with density and volume such that:

$$m_i = V_i \cdot \rho = l_i \cdot A_i \cdot \rho_i \quad (9)$$

Where l_i and A_i denote the length and area of the layer, respectively. Coming back to expression (7) we finally obtain:

$$c_p = \sum_i \frac{l_i \cdot A_i \cdot \rho_i \cdot c_p^i}{\sum_j l_j \cdot A_j \cdot \rho_j} \quad (10)$$

As the area is equal for each layer we can extract it from the sumatory, resulting in:

$$c_p = \sum_i \frac{l_i \cdot \rho_i \cdot c_p^i}{\sum_j l_j \cdot \rho_j} \quad (11)$$

Using this final expression, as well as the expressions (5) and (6), with the auxilaray use of Tables 5.1 and 5.2, we compute these variables:

PCB	c_p [J/kg · K]	$k_{c,p}$ [W/m · K]	$k_{i,p}$ [W/m · K]
OBC-COMMS	940	0.32	91
EPS	940	0.32	91
ADCS	940	0.32	91
Y+Mag	904	0.32	171
Laterals	904	0.32	171
Bottom	904	0.32	171
Slider	1050	0.30	47
Kband Under	783	0.31	110
Kband Over (Antenna)	905	0.29	89

Table 5.3: PCB Bulk Thermal Properties

5.1.4 Introduction to the GMM

The modelling of the spacecraft will be presented in ascending order, grouping geometries in the same section by logical relation. As there isn't a structure acting as the skeleton of the PocketQubes, no section is reserved to it.

Before this, though, a general overview of the model is given . In Figure 5.3 an exploded view of PoCat-3 is presented, highlighting some its most important components.

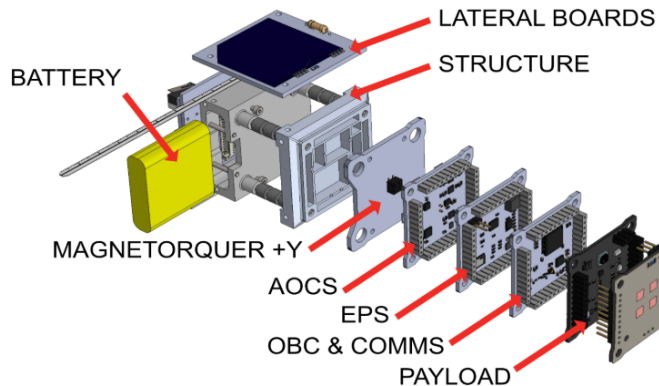
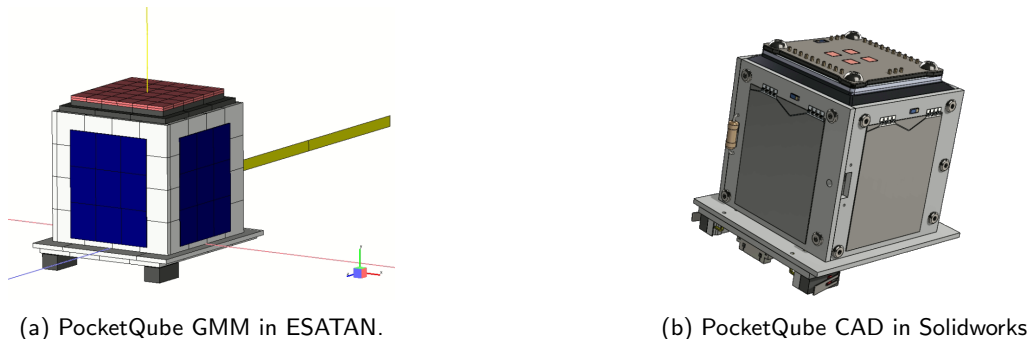


Figure 5.3: Exploded view of the PoCat-3 spacecraft.

Some views of the CAD model used as a reference for the creation of geometries in ESATAN are presented next in contrast to the actual geometries modeled for the thermal analysis:

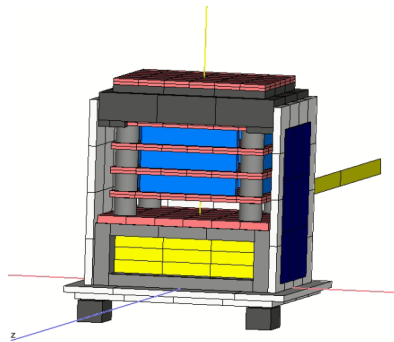


(a) PocketQube GMM in ESATAN.

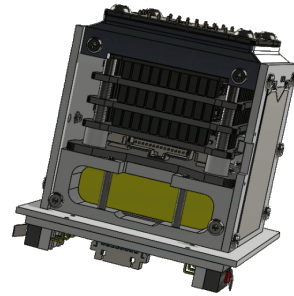
(b) PocketQube CAD in Solidworks

Figure 5.4: Full GMM in ESATAN and in Solidworks.

Removing a lateral board in order to get a better view into the PocketQube:



(a) PocketQube GMM in ESATAN w/o a lateral board.



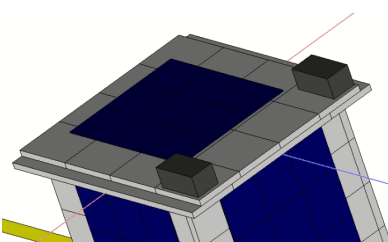
(b) PocketQube GMM in Solidworks w/o a lateral board.

Figure 5.5: PocketQube GMM in ESATAN and Solidworks w/o a lateral board.

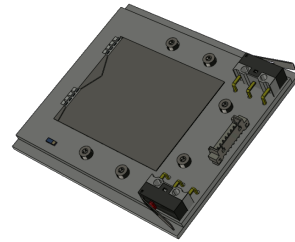
5.1.5 Killswitches

The killswitches act as the interruptor enabling power of the spacecraft as it is released into orbit. They are mainly composed by main rectangular body, where the internal circuitry is located, covered by a black plastic case, the levers, that serve as the actuators of the interruptor, and the legs that connect to the bottom board.

Considering the small crosssection of the levers and the legs, the killswitches are geometrically modeled as a simple solid rectangular prism. The visual representation and comparison with the CAD is presented next:



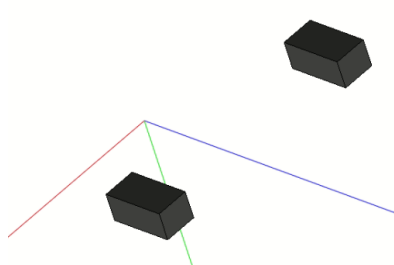
(a) Killswitches in ESATAN (with other components)



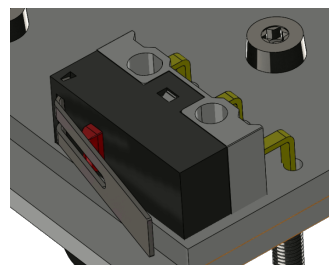
(b) Killswitches in Solidworks (with other components)

Figure 5.6: Comparison between thermal and CAD model for the Killswitches (with other components).

Providing a close-up into the killswitches:



(a) Killswitches in ESATAN (without other components)



(b) Killswitches in Solidworks (without other components)

Figure 5.7: Comparison between thermal and CAD model for the Killswitches (without other components)

The properties of the killswitches themselves, as determined by following the procedure specified in this section are:

<i>SD_KS_PX</i>	Material	m (g)	m (kg)	m(%)	V_E [m³]	ρ [kg/m³]	c_p [J/kg · K]	k_{c,p.}[W/m · K]	k_{i,p.}[W/m · K]
<i>Primitive</i>	ABS	1.2	0.0012	100	4.56E-07	2632	1990	0.162	0.162
<i>Idem</i>									
<i>SD_KS_NX</i>	ABS	1.2	0.0012	100	4.56E-07	2632	1990	0.162	0.162

Table 5.4: Bulk properties of the killswitches.

The optical properties:

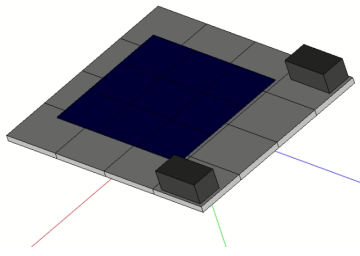
Primitive	Material	ϵ_{IR}	α_S
<i>SD_KS_PX</i>	ABS	0.82	0.94

Table 5.5: Optical properties of the killswitches primitives.

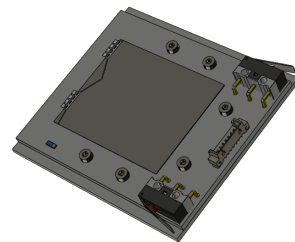
5.1.6 Bottom Board

The bottom board hosts some screws, a solar panel (SP-Y) and the killswitches. It is a four copper layer PCB with a magnetorquer ingrained into it. It is made of a total of nine layers, four copper layers, three FR-4, and two solder masks (black).

It is modeled as a solid orthotropic rectangular prism, with the bulk properties as specified in Table 5.4 and with the optical properties of white paint as specified in Table 5.1. The components other than the PCB itself are only considered in the calculation of density, yet ignored for the specific heat and conductivity. The visual representation and comparison with the CAD is presented next:



(a) Bottom PCB in ESATAN



(b) Bottom PCB in Solidworks

Figure 5.8: Comparison between thermal and CAD model for the Bottom Board.

The bulk properties of the primitive:

<i>SD_Bottom_Board</i>	Material	m (g)	m (kg)	m(%)	V_E[m³]	ρ[kg/m³]	c_p[J/kg · K]	k_{c,p.}[W/m · K]	k_{i,p.}[W/m · K]
<i>Bottom PCB</i>	Bottom PCB	14.2	1.42E-02	100	x	2133	904	0.32	170.88
<i>Primitive</i>	Bottom PCB	14.2	1.42E-02	100	6.66E-06	2133	904	0.32	170.88

Table 5.6: Bulk properties of the bottom PCB.

The optical properties:

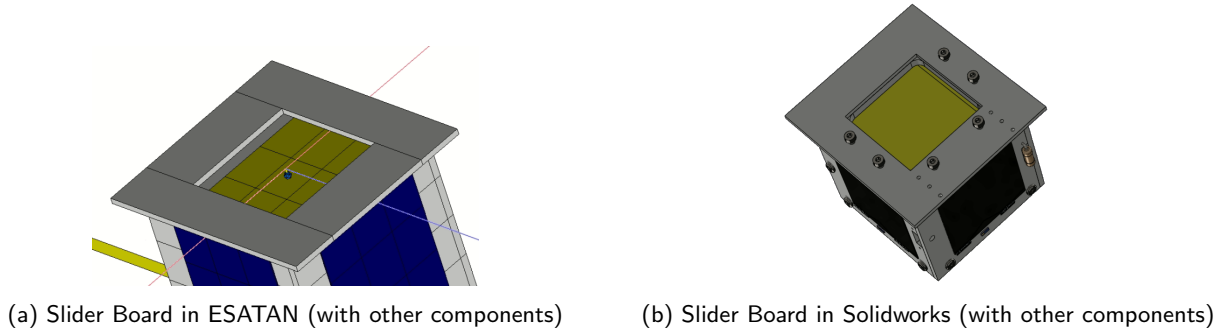
Primitive	Material	ϵ_{IR}	α_S
<i>SD_Bottom_Board</i>	White Paint	0.94	0.19

Table 5.7: Optical properties of the bottom board primitive.

5.1.7 Slider Board

The slider board is placed directly over the bottom board. It is the support where the lateral boards rest. Its purpose is to allow the deployment of the PocketQube by the sliding of the S/C over a rail, in the deployer. It is also a PCB, made of two layers of copper, one of FR-4 and two of solder mask, set to white.

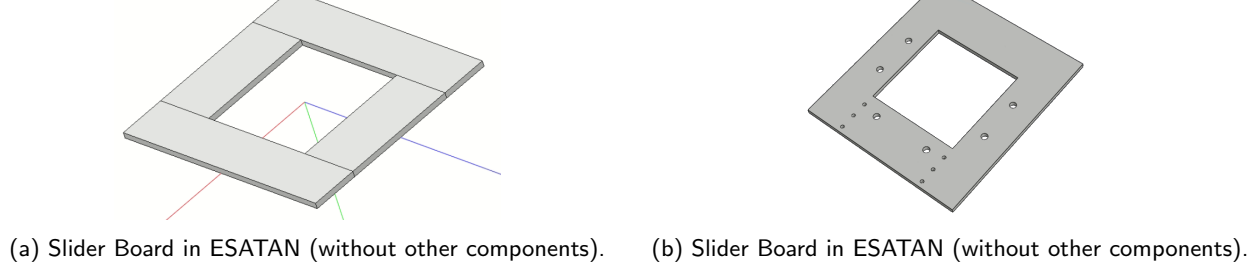
The most distinctive characteristic of the slider board is the fact that it presents a rectangular shaped hole in the middle of itself. This results in a slightly more complex modeling, leading to the division of the PCB into 4 smaller primitives. The visual representation and comparison with the CAD is presented next:



(a) Slider Board in ESATAN (with other components) (b) Slider Board in Solidworks (with other components)

Figure 5.9: Comparison between thermal and CAD model for the Slider Board (with other components)

An isolated view:



(a) Slider Board in ESATAN (without other components). (b) Slider Board in ESATAN (without other components).

Figure 5.10: Comparison between thermal and CAD model for the Slider Board (without other components)

The properties of the primitives:

Slider Board	Material	m (g)	m (kg)	m(%)	$V_E[m^3]$	$\rho[\text{kg}/\text{m}^3]$	$c_p[\text{J}/\text{kg} \cdot \text{K}]$	$k_{c.p.}[\text{W}/\text{m} \cdot \text{K}]$	$k_{i.p.}[\text{W}/\text{m} \cdot \text{K}]$
Real Slider	PCB	8.4	8.40E-03	x	x	x	x	x	x
SD_Slider_Board									
SD_Slider_L	Slider	x	x	31	1.33E-06	1953	1050	0.30	46.76
SD_Slider_R	Slider	x	x	31	1.33E-06	1953	1050	0.30	46.76
SD_Slider_Front	Slider	x	x	19	8.19E-07	1953	1050	0.30	46.76
SD_Slider_Back	Slider	x	x	19	8.19E-07	1953	1050	0.30	46.76
<i>Total</i>	Slider	8.4	8.40E-03	100	4.30E-06	1953	1050	0.30	46.76

Table 5.8: Slider board primitives bulk properties. Mass percentage is calculated by volume and density.

The optical properties:

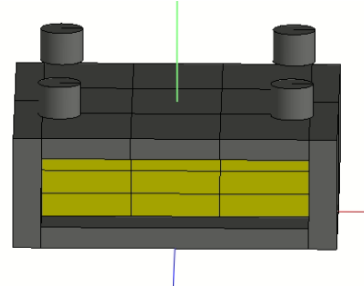
Primitive	Material	ϵ_{IR}	α_s
SD_Slider_Board_X	White Paint	0.94	0.14

Table 5.9: Optical properties of the slider board primitives.

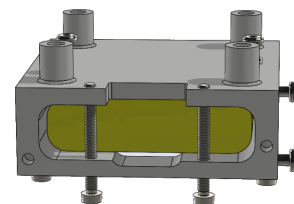
5.1.8 Battery and Battery Support (Case)

The battery is a LiPo 1400mAh battery, contained within a case made of PTFE, so as to guarantee its security and minimize risk of debris in case of a catastrophic failure. This support is also where the magnetorquer +Y PCB lies, leading to the start of the PCB stack.

The battery is simply modeled as a solid rectangular prism while, in a similar fashion as with the slider board, the support geometry is sliced into different primitives, solid rectangular prisms and solid cylinders on top of it. The visual representation and comparison with the CAD is presented next:



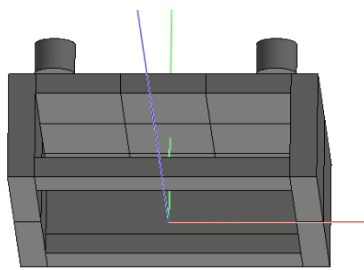
(a) Battery Support in ESATAN (with battery).



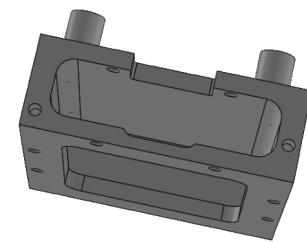
(b) Battery Support in Solidworks (with battery).

Figure 5.11: Comparison between thermal and CAD model for the Battery Support (with battery)

An isolated view, without the battery placed inside:



(a) Battery Support in ESATAN (without battery).



(b) Battery Support in Solidworks (without battery).

Figure 5.12: Comparison between thermal and CAD model for the Battery Support (without battery)

The properties of the primitives:

SD_Battery	Material	m (g)	m (kg)	m(%)	V _E [m ³]	ρ [kg/m ³]	c _p [J/kg · K]	k _{c,p} [W/m · K]	k _{i,p} [W/m · K]
Primitive	LiPo Battery	34	3.40E-02	100	1.22E-05	2796	1000	0.60	2.50

Table 5.10: Bulk properties of the battery.

Battery Support	Material	m (g)	m (kg)	m(%)	V _E [m ³]	ρ [kg/m ³]	c _p [J/kg · K]	k _{c,p} [W/m · K]	k _{i,p} [W/m · K]
Real Support	PTFE	30	3.00E-02	100	x	x	x	x	x
SD_BottStruc									
SD_BottStruc_BackMid	PTFE*	x	x	x	2.66E-06	1886	1010	0.27	0.27
SD_BottStruc_DownBack	PTFE*	x	x	x	7.98E-07	1886	1010	0.27	0.27
SD_BottStruc_DownFront	PTFE*	x	x	x	7.98E-07	1886	1010	0.27	0.27
SD_BottStruc_L	PTFE*	x	x	x	2.94E-06	1886	1010	0.27	0.27
SD_BottStruc_R	PTFE*	x	x	x	2.94E-06	1886	1010	0.27	0.27
SD_BottStruc_Up	PTFE*	x	x	x	5.24E-06	1886	1010	0.27	0.27
SD_BattSuppSpacer_1	PTFE**	0.302	3.02E-04	x	1.30E-07	4207	500	15	15.00
Spacer	PTFE	0.00024516	2.45E-07	< 1	x	2070	1010	0.27	0.27
Screw	AISI304SS	0.30175	3.02E-04	> 99	x	8000	500	15	15
Idem									
SD_BattSuppSpacer_2	PTFE**	0.302	3.02E-04	x	1.30E-07	4207	500	15	15.00
SD_BattSuppSpacer_3	PTFE**	0.302	3.02E-04	x	1.30E-07	4207	500	15	15.00
SD_BattSuppSpacer_4	PTFE**	0.302	3.02E-04	x	1.30E-07	4207	500	15	15.00
Total (BottStruc)	PTFE(*)(**)	30	3.00E-02	100	1.59E-05	1886	1010	0.27	0.27

Table 5.11: Battery support primitives bulk properties.*Adjusted density to ESATAN volume.**Considering the screw inside.

The optical properties:

Primitive	Material	ϵ_{IR}	α_s
SD_Battery	LiPo Battery	0.3	0.5

Table 5.12: Optical properties of the LiPo Battery.

Primitive	Material	ϵ_{IR}	α_s
SD_BattXX_XX	PTFE	0.92	0.046

Table 5.13: Optical properties of the battery support.

5.1.9 Vertical Connectors

The vertical connectors link the stack PCBs to each other, distributing both power and data lines. They are rectangular plastic pieces, with phosphor bronze metallic contacts that protrude out of them.

In order to model them in a simple manner, they are considered solid rectangular prisms with the average properties of the plastic and the phosphor bronze connectors.

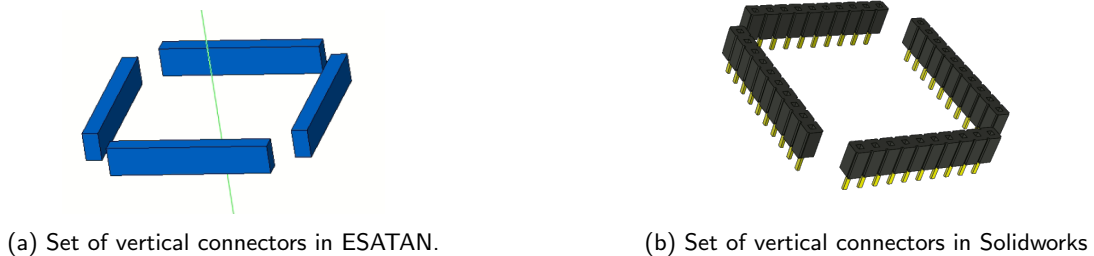


Figure 5.13: Comparison between thermal and CAD model of the vertical connectors.

The bulk properties assigned to them are:

SD_JXSSySSz_VC	Material	m (g)	m (kg)	m(%)	$V_E[m^3]$	$\rho[kg/m^3]$	$c_p[J/kg \cdot K]$	$k_{c,p.}[W/m \cdot K]$	$k_{i,p.}[W/m \cdot K]$
Inner Connector	Phosphor Bronze	0.325	3.25E-04	45	x	8800	380	62.00	62.00
Plastic Cover	ABS	0.4	4.00E-04	55	x	1070	1990	0.16	0.16
Primitives	Bulk VC (Custom)	0.725	7.25E-04	100	2.90E-07	2502	1268	27.88	27.88

Table 5.14: Bulk properties of the vertical connectors primitives.

The optical properties of the vertical connectors are:

Primitive	Material	ϵ_{IR}	α_s
SD_JXSSySSz_VC	ABS	0.82	0.94

Table 5.15: Optical properties of the vertical connectors.

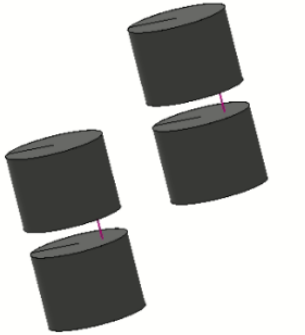
5.1.10 Spacers

The spacers used are threaded by screws that run from the top PCB of the payload to the battery support. Their purpose is to, as their name indicates, provide a specific space between the PCBs.

The actual spacers are closer to tubes than to cylinders, but are modeled as the later in order to keep the model simple. This does pose an issue, as the screws cannot be modeled running through them. Instead, they are considered when calculating the bulk properties of the volume and ignored geometrically.

The spacers are also connected by UDC in order to represent this lost conductivity provided by the screws.

Some views of the pieces and models:



(a) Set of spacers connected by UDCs.



(b) Spacer threaded by a screw.

Figure 5.14: Comparison of spacers in ESATAN and in Solidworks.

The bulk properties of the spacers are:

SD_Spacer_SStoSSx	Material	m (g)	m (kg)	m(%)	V _E [m ³]	ρ [kg/m ³]	c _p [J/kg · K]	k _{c,p} [W/m · K]	k _{i,p} [W/m · K]
M3x35 Hex (Partial)	AISI304SS	0.30175	3.02E-04	51	x	x	500	15	15.00
M3x4 Spacer (Fully)	AISI304SS	0.22	2.20E-04	37	x	x	500	15	15.00
M3x0.5 Spacer (Fully)	6063-T5	0.07	7.00E-05	12	x	x	900	209	209.00
Primitives	Spacer Custom	0.59175	5.92E-04	1	1.30E-07	4552	547	15	15.00

Table 5.16: Bulk properties of the spacers primitives.

The optical properties of the spacers:

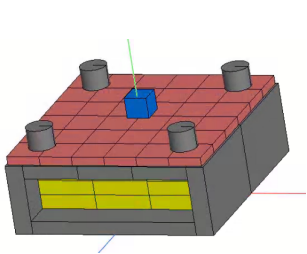
Primitive	Material	ϵ_{IR}	α_s
SD_Spacer_SStoSSx	AISI304SS	0.075	0.42

Table 5.17: Optical properties of the spacers.

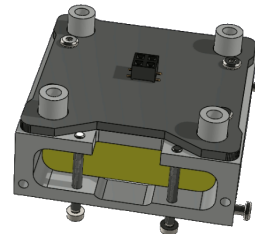
5.1.11 Magnetorquer +Y

The +Y magnetorquer is placed on the bottom of the PCB stack, directly resting over the battery support. As is the case with the other magnetorquers, its purpose is to provide rotation to the PQ in order to control its attitude.

Despite it having four holes in each one of its corners, in the actual spacecraft, it has been modeled as a solid rectangular prism without them. Some small components placed on top of the board have been ignored to simplify the model. The visual representation and comparison with the CAD is presented next:



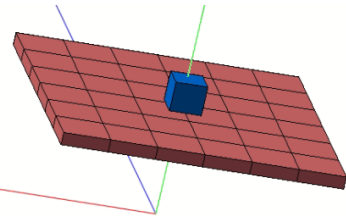
(a) MTQ +Y Model in ESATAN (Top View)



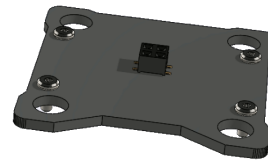
(b) MTQ +Y Model in Solidworks (Top View)

Figure 5.15: Comparison between thermal and CAD model for the MTG +Y (Top View)

An isolated view:



(a) MTQ +Y Model in ESATAN (Isolated View)



(b) MTQ +Y Model in Solidworks (Isolated View)

Figure 5.16: Comparison between thermal and CAD model for the MTG +Y (Isolated View)

The bulk properties of the primitives:

SD_MTQ_PY_Board	Material	m (g)	m (kg)	m(%)	V_E[m^3]	$\rho[\text{kg}/\text{m}^3]$	$c_p[\text{J}/\text{kg} \cdot \text{K}]$	$k_{c,p}[\text{W}/\text{m} \cdot \text{K}]$	$k_{i,p}[\text{W}/\text{m} \cdot \text{K}]$
MTQ PY PCB	Y+Mag	6.6	6.60E-03	93	x	1630	904	0.45	170.88
Components	Y+Mag	0.5	5.00E-04	7	x	1630	904	0.45	170.88
Total	Y+Mag	6.6	6.60E-03	100	4.05E-06	1630	904	0.45	170.88

Table 5.18: Bulk properties of the magnetorquer (Positive Y axis) primitive.

The optical properties of the MTQ+Y:

Primitive	Material	ϵ_{IR}	α_S
SD_MTQ_PY_Board	Black Coat	0.94	0.96

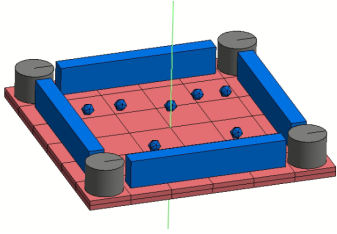
Table 5.19: Optical properties of the MTQ+Y.

5.1.12 Attitude and Orbit Determination and Control

The AOCS subsystem is centralized and operated within the AOCS PCB. This PCB is placed directly over the MTQ +Y board, held by the spacers on top of the battery support. It houses different electrical components as well as the vertical connectors linking the subsystem with the OBC-COMMS PCB.

As will be the approach taken with the rest of the stack PCBs, the holes on the four corners have been not modeled, instead representing the AOCS PCB by a solid rectangular prism. It is in contact with a total of eight vertical connectors, four on each face. It is also in contact with the PCB spacers. The ICs are modeled as Non-Geometrical Thermal Nodes, placed on top of the PCB.

The visual representation and comparison with the CAD is presented next:



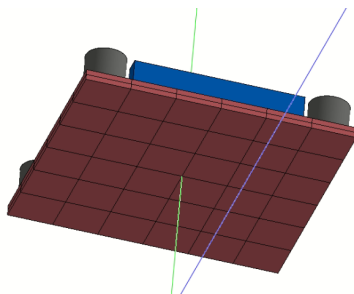
(a) AOCS Model in ESATAN (Top View)



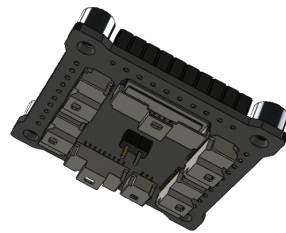
(b) AOCS Model in Solidworks (Top View)

Figure 5.17: Comparison between thermal and CAD model for the AOCS (Top View)

A bottom view:



(a) AOCS Model in ESATAN (Bottom View)



(b) AOCS Model in Solidworks (Bottom View)

Figure 5.18: Comparison between thermal and CAD model for the AOCS (Bottom View).

The bulk properties of the primitive:

SD_AOCS_Board	Material	m (g)	m (kg)	m(%)	V _E [m ³]	ρ [kg/m ³]	c _p [J/kg · K]	k _{c,p} [W/m · K]	k _{i,p} [W/m · K]
AOCS PCB	AOCS	5.6	5.60E-03	70	x	3125	940	0.42	91.47
Components	AOCS	2.4	2.40E-03	30	x	3125	940	0.42	91.47
Primitive	AOCS	8	8.00E-03	100	2.56E-06	3125	940	0.42	91.47

Table 5.20: Bulk properties of the AOCS board.

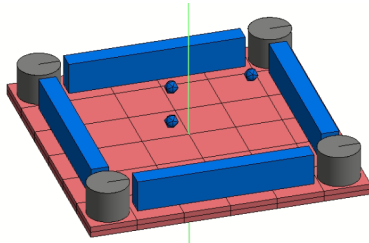
Primitive	Material	ϵ_{IR}	α_S
SD_AOCS_Board	Black Coat	0.94	0.96

Table 5.21: Optical properties of the AOCS PCB primitive.

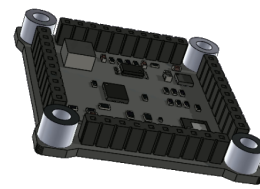
5.1.13 Electrical Power Supply

The EPS is the subsystem tasked with power gathering, distribution and management, including battery monitoring. The PCB itself houses the MPPTs and ICs to perform the aforementioned functions. The EPS PCB is modeled as a solid rectangular prism and the ICs as NGTN. It is in contact with a total of eight vertical connectors, four on each face and with the PCB spacers.

The visual representation and comparison with the CAD is presented next:



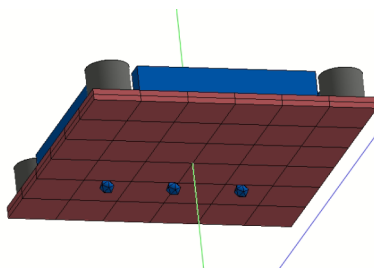
(a) EPS Model in ESATAN (Top View)



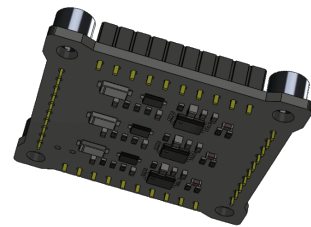
(b) EPS Model in Solidworks (Top View)

Figure 5.19: Comparison between thermal and CAD model for the EPS (Top View)

A bottom view:



(a) EPS Model in ESATAN (Bottom View)



(b) EPS Model in Solidworks (Bottom View)

Figure 5.20: Comparison between thermal and CAD model for the EPS (Bottom View).

The bulk properties of the EPS board:

SD_EPS_Board	Material	m (g)	m (kg)	m(%)	V _E [m ³]	ρ [kg/m ³]	c _p [J/kg · K]	k _{c.p.} [W/m · K]	k _{i.p.} [W/m · K]
EPS PCB	EPS	5.5	5.50E-03	77	x	2773	940	0.42	91.47
Components	EPS	1.6	1.60E-03	23	x	2773	940	0.42	91.47
Primitive	EPS	7.1	7.10E-03	100	2.56E-06	2773	940	0.42	91.47

Table 5.22: Bulk properties of the EPS board primitive.

The optical properties of the EPS PCB primitive:

Primitive	Material	ϵ_{IR}	α_S
SD_EPS_Board	Black Paint	0.94	0.96

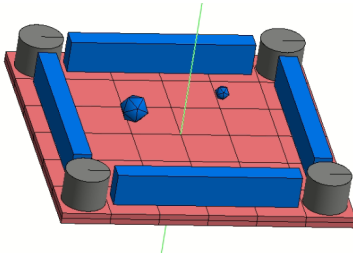
Table 5.23: Optical properties of the EPS PCB primitive.

5.1.14 On Board Computer and Communications

The On-Board Computer and the Communications subsystems are both housed by the same PCB, at the center of the stack. The OBC subsystem is tasked with the processing of data and management of the other subsystems. The COMMS subsystem performs the sending and reception of RF signals containing data such as telemetry, payload data and telecommands.

The PCB model follows the same philosophy as the other stack PCBs and is in contact with the same number of vertical connectors and spacers as the others. It is then modeled as a solid rectangular prisms with NGTN as ICs, including in this case, of most relevance, the processor (STM32).

The visual representation and comparison with the CAD is presented next:



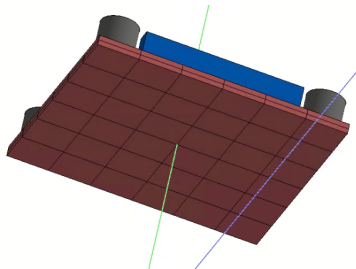
(a) OBC and COMMS Model in ESATAN (Top View)



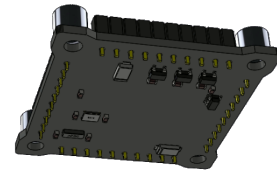
(b) OBC and COMMS Model in Solidworks (Top View)

Figure 5.21: Comparison between thermal and CAD model for the OBC and COMMS Model (Top View)

A bottom view:



(a) OBC and COMMS Model in ESATAN (Bottom View)



(b) OBC and COMMS Model in Solidworks (Bottom View)

Figure 5.22: Comparison between thermal and CAD model for the OBC and COMMS Model (Bottom View)

The bulk properties of the OBC primitive:

SD_OBC_Board	Material	m (g)	m (kg)	m(%)	V_E[m^3]	$\rho[\text{kg}/\text{m}^3]$	$c_p[\text{J}/\text{kg} \cdot \text{K}]$	$k_{e,p.}[\text{W}/\text{m} \cdot \text{K}]$	$k_{i,p.}[\text{W}/\text{m} \cdot \text{K}]$
OBC COMMS PCB Components	OBC COMMS	5.4	5.40E-03	77	x	2734	940	0.42	91.47
Primitive	OBC COMMS	1.6	1.60E-03	23	x	2734	940	0.42	91.47
	OBC COMMS	7	7.00E-03	100	2.56E-06	2734	940	0.42	91.47

Table 5.24: Bulk properties of the OBC-COMMS PCB primitive.

The optical properties of the OBCCOMMS PCB primitive:

Primitive	Material	ϵ_{IR}	α_S
SD_OBC_Board	Black Coat	0.94	0.96

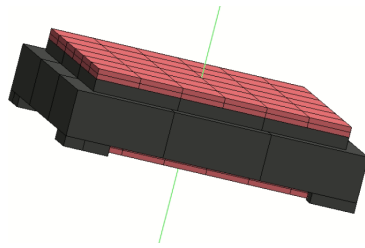
Table 5.25: Optical properties of the OBCCOMMS PCB primitive.

5.1.15 Payload (K-Band)

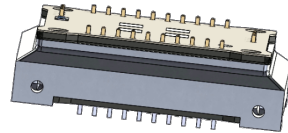
The K-Band payload consists of two PCBs, one located directly over the OBC-COMMS PCB and the other placed on top of an aluminum support. Over this second PCB is located a 4-patch array antenna. The objective of the payload is to gather radiometry measurements in this band.

The modelling in this case will be split into three different main parts: the bottom PCB, the K-Band Support and the top PCB with the antenna. The PCBs are modeled as solid rectangular prisms, with NGTNs replacing the ICs. For the K-Band support different rectangular prisms have been combined in order to create a structure as close to the real one as possible.

Different views of the payload and the support are provided next:

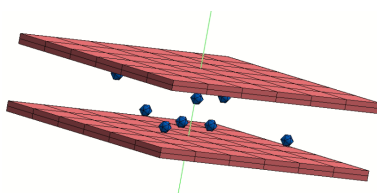


(a) Isolated view of the K-Band P/L in ESATAN.

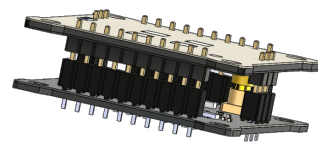


(b) Isolated view of the K-Band P/L in Solidworks.

Figure 5.23: Comparison between thermal and CAD model for the K-Band Payload.

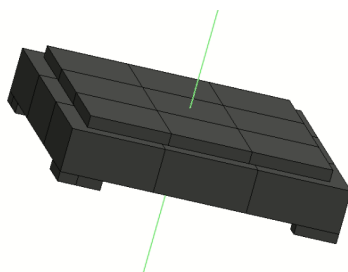


(a) Isolated view of the K-Band P/L in ESATAN w/o support.

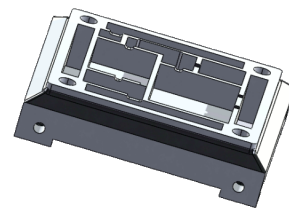


(b) Isolated view of the K-Band P/L in Solidworks w/o support.

Figure 5.24: Comparison between thermal and CAD model for the K-Band Payload without support,

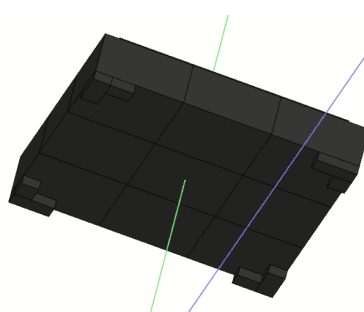


(a) Isolated view of the K-Band P/L support in ESATAN.

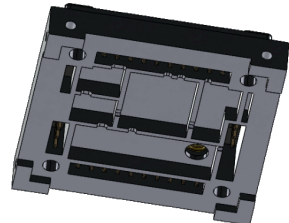


(b) Isolated view of the K-Band P/L support in Solidworks.

Figure 5.25: Comparison between thermal and CAD model for the K-Band Payload support.



(a) Isolated bottom view of the K-Band P/L support in ESATAN.



(b) Isolated bottom view of the K-Band P/L support in Solidworks.

Figure 5.26: Comparison between thermal and CAD model for the K-Band Payload support (bottom view).

As it can be seen, the support has been heavily simplified, leaving the model without vertical connectors from the top PCB to the bottom PCB. In future iterations the modeling of this conductivity might be considered.

The bulk properties of both PCBs are:

SD_PL_Board	Material	m (g)	m (kg)	m(%)	V_E[m³]	ρ[kg/m³]	c_p[J/kg · K]	k_{c,p} [W/m · K]	k_{i,p} [W/m · K]
P/L Under PCB + Components Primitive	KBand Under KBand Under	9.2 9.2	9.20E-03 9.20E-03	100 100	x 2.56E-06	3594 3594	783 783	0.49 0.49	110.15 110.15

Table 5.26: Bulk properties of the P/L Under PCB.

SD_PLAntenna_Board	Material	m (g)	m (kg)	m(%)	V_E[m³]	ρ[kg/m³]	c_p[J/kg · K]	k_{c,p} [W/m · K]	k_{i,p} [W/m · K]
P/L Top PCB + Components Antenna Primitive	Kband Over Kband Over Kband Over	7.6 0.7 8.3	7.60E-03 7.00E-04 8.30E-03	91 9 100	x x 2.56E-06	3242 3242 3242	905 905 905	0.29 0.29 0.29	88.53 88.53 88.53

Table 5.27: Bulk properties of the P/L Top (+Antenna) PCB. The antenna properties are assumed to be the same as for the PCB (approximation).

When it comes to the K-Band support itself, the screws that run through it are considered (by the amount of volume overlapping the defined primitive) to determine the bulk properties.

K-Band Support	Material	m (g)	m (kg)	m(%)	V_E[m³]	ρ[kg/m³]	c_p[J/kg · K]	k_{c,p} [W/m · K]	k_{i,p} [W/m · K]
Real Support Screws Crossing (0.29* 4)	Alloy 7075 AISI304SS	24 1.972	2.40E-02 1.97E-03	92 8	x x	x 8000	960 500	130.00 15.00	130.00 15.00
SD_PLSupp									
SD_PLSupp.Top	x	x	x	x	3.12E-06	1401	925	121.27	121.27
SD_PLSupp.Mid	x	x	x	x	1.52E-05	1401	925	121.27	121.27
SD_PLSupp.Aux1a	x	x	x	x	3.36E-08	1401	925	121.27	121.27
SD_PLSupp.Aux1b Idem	x	x	x	x	1.92E-08	1401	925	121.27	121.27
SD_PLSupp.AuxXY	x	x	x	x	x	1401	925	121.27	121.27
Total	KBand Support Custom	25.972	2.60E-02	100	1.85E-05	1401	925	121.27	121.27

Table 5.28: Bulk properties of the K-Band Support.

The optical properties of these PCBs and support are:

Primitive	Material	ε_{IR}	α_S
SD_PL_Board	Black Coat	0.94	0.96
SD_PLAntenna_Board	Black Coat	0.94	0.96
SD_PLSupp_XX	Aluminum 6063-T5	0.77	0.80

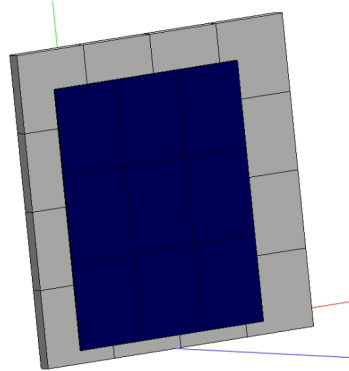
Table 5.29: Optical properties of the K-Band payload.

5.1.16 Lateral Boards and Solar Panels

The lateral boards are equipped with different sensors such as photodiodes and temperature sensors, and, most importantly, hold the solar panels that power the PQ. One of them also holds a thermal knife that will be used to melt a dynnema, releasing the COMMS Antenna.

They are modeled by solid rectangular prisms. On one face of these prisms is located another rectangular prism which represents the solar panels.

Some views to illustrate the modelling are provided next:

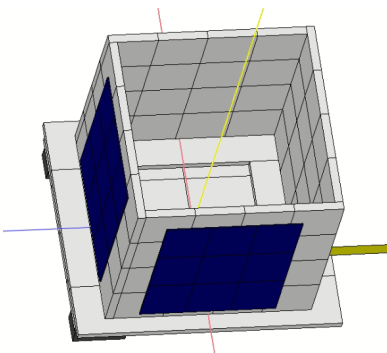


(a) Lateral Board with Solar Panel in ESATAN.

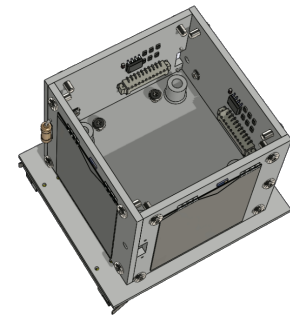


(b) Lateral Board with Solar Panel in Solidworks.

Figure 5.27: Comparison between thermal and CAD model for the lateral boards.



(a) Empty PQ view in ESATAN.



(b) Empty PQ view in Solidworks.

Figure 5.28: Comparison between thermal and CAD model of an empty PQ.

The bulk properties of the lateral boards and solar panels primitives:

SD_PX_Lateral_Board	Material	m (g)	m (kg)	m(%)	V_E[m³]	ρ[kg/m³]	c_p[J/kg · K]	k_{c,p} [W/m · K]	k_{i,p} [W/m · K]
PX PCB Components	BotLat Bulk N/A	9.8 0.4	9.80E-03 4.00E-04	96 4	x x	2214 2214	904 904	0.45 0.45	170.88 170.88
<i>Primitive Idem</i>	-	10.2	1.02E-02	100	4.61E-06	2214	904	0.45	170.88
SD_NZ_Lateral_Board		10.2	1.02E-02	100	4.61E-06	2214	904	0.45	170.88
SD_PZ_Lateral_Board		10.2	1.02E-02	100	4.61E-06	2214	904	0.45	170.88
NX PCB Components(+TK)	BotLat Bulk N/A	9.8 0.6	9.80E-03 6.00E-04	94 6	x x	2257 2257	904 904	0.45 0.45	170.88 170.88
SD_NX_Lateral_Board	-	10.4	1.04E-02	100	4.61E-06	2257	904	0.45	170.88

Table 5.30: Bulk properties of the lateral boards.

SD_SP_PX_Board	Material	m (g)	m (kg)	m(%)	V_E[m³]	ρ[kg/m³]	c_p[J/kg · K]	k_{c,p} [W/m · K]	k_{i,p} [W/m · K]
<i>Total Idem</i>	GaAs	0.9	9.00E-04	100	3.96E-07	2273	325	50	50.00
SD_SP_NX_Board	GaAs	0.9	9.00E-04	100	3.96E-07	2273	325	50	50.00
SD_SP_NY_Board	GaAs	0.9	9.00E-04	100	3.96E-07	2273	325	50	50.00
SD_SP_PZ_Board	GaAs	0.9	9.00E-04	100	3.96E-07	2273	325	50	50.00
SD_SP_NZ_Board	GaAs	0.9	9.00E-04	100	3.96E-07	2273	325	50	50.00

Table 5.31: Bulk properties of the solar panels.

The optical properties of the lateral boards and solar panels:

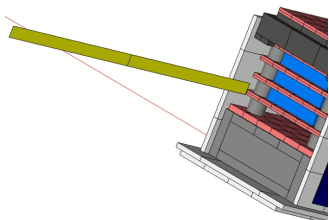
Primitive	Material	ϵ_{IR}	α_S
SD_-±X/Y/Z_Lateral_Board	White Paint	0.94	0.19
SD_SP_-±X/Y/Z	Gallium Arsenide	0.85	0.91

Table 5.32: Optical properties of the lateral boards and the solar panels.

5.1.17 COMMS Antenna

The COMMS Antenna is a $\lambda/4$ monopole tuned to a frequency of 868MHz. It transmits and receives RF signals to and from the ground station. It is soldered and screwed into a lateral board, which in turn is connected to the COMMS PCB.

The COMMS Antenna is modeled as a solid rectangular prism connected with a UDC to a lateral board.



(a) COMMS Antenna model in ESATAN.



(b) PoCat-1 image.

Figure 5.29: Comparison between thermal model and image of the COMMS Antenna.

The bulk properties of the antenna are:

SD_COMMS_Antenna	Material	m (g)	m (kg)	m(%)	V _E [m ³]	ρ [kg/m ³]	c _p [J/kg · K]	k _{e,p} [W/m · K]	k _{i,p} [W/m · K]
Primitive	AISI304SS	5.7	5.70E-03	100	7.13E-07	8000	500	15	15

Table 5.33: Bulk properties of the COMMS Antenna.

And the optical properties:

Primitive	Material	ϵ_{IR}	α_S
SD_COMMS_Antenna	AISI304SS	0.075	0.42

Table 5.34: Optical properties of the COMMS antenna.

5.2 NGTNs and User Defined Conductors

The use of user defined conductors (UDC) has been implemented in order to better represent the heat flow from the spacers, the ICs and the antenna. The further use of GLs might be studied in further iterations.

5.2.1 Non-Geometrical Thermal Nodes

As has been mentioned in the previous subsection, the use of Non-Geometrical Thermal Nodes to represent the ICs in each stack PCB relies in the definition of GLs from said nodes to the nodes of the PCB mesh. Therefore, for each IC, depending on its package, a value of conductance has been set.

These values have been extracted from similar ICs empirical resistance due to the lack of junction to case resistance information. Also, as this measure is defined only to compare between ICs and doesn't provide any standalone value, it has been further seen fit to extract the values in this manner. Do note that the values taken are order of magnitude approximations.

A list of the conductances for NGTNs is provided next:

ESATAN Name	Component	Package	$\Theta_{JB}(K/W)$	G (W/K)
NGTN_ADCS_U1	LPV542	X1SON	20	0.05
NGTN_ADCS_U2	LPV542	X1SON	20	0.05
NGTN_ADCS_U3	LPV542	X1SON	20	0.05
NGTN_ADCS_U4	IIM-42652	14-pin LGA	15	0.07
NGTN_ADCS_U5	BD2606MVV	SQFN016V4040	5	0.20
NGTN_ADCS_U6	TMUX1108RSVR	RSV (QFN, 16)	5	0.20
NGTN_ADCS_U7	MMC5983MA	ILSP	15	0.07
NGTN_Batt_Heater	x	x	x	x
NGTN_EPS_IC1	DS2782E+	TDFN-10	10	0.10
NGTN_EPS_IC2	ISL9120IRTNZ	TQFN	10	0.10
NGTN_EPS_U1	SPV1040TTR	TSSOP8	15	0.07
NGTN_EPS_U2	SPV1040TTR	TSSOP8	15	0.07
NGTN_EPS_U3	SPV1040TTR	TSSOP8	15	0.07
NGTN_EPS_U4	LTC4040EUFD#PBF	QFN	5	0.20
NGTN_OBC_STM32	STM32L476RGTx	LQFP - 64 pins	10	0.10
NGTN_OBC_SX1262	SX1262IMLRT	QFN (24L)	5	0.20
NGTN_PLTOP_U1	HMC342LC4	SMT	5	0.20
NGTN_PLTOP_U2	HMC516LC5	SMT	5	0.20
NGTN_PLTOP_Y1	HMC506LP4ETR	QFN Leadless SMT	5	0.20
NGTN_PLUNDER_U1	CMD271P3	QFN Package	5	0.20
NGTN_PLUNDER_U2	SIM-14+	HV1195	5	0.20
NGTN_PLUNDER_U3	LT5537EDDB#TRMPBF	DFN (8L)	10	0.10
NGTN_PLUNDER_U4	LEE2-6+	MC1630-1 (6L)	15	0.07
NGTN_PLUNDER_U5	LEE2-6+	MC1630-1 (6L)	15	0.07
NGTN_PLUNDER_U7	HMC358MS8GE	MSOP8G SMT	15	0.07

Table 5.35: NGTNs UDC assigned values.

5.2.2 Spacers

Due to the lack of the modelling of holes in the PCBs, it is to be expected that the top to bottom conductivity of the PCB stack is reduced. In order to mitigate this effect, user defined conductors have been placed between each one of the spacers of the stack, with the conductance set to that of stainless steel. Note that this is a first approximation and a more detailed mathematical model might be needed to correlate experimental results.



Figure 5.30: Spacers with GLs between them in ESATAN.

5.2.3 Antenna

The COMMS antenna is soldered and screwed to the interior surface of a lateral board. The conductance of the contact has been modeled as if a square centimeter of the antenna was in contact with the lateral board, with the conductivity of tin, as it is the material it is soldered and covered with.

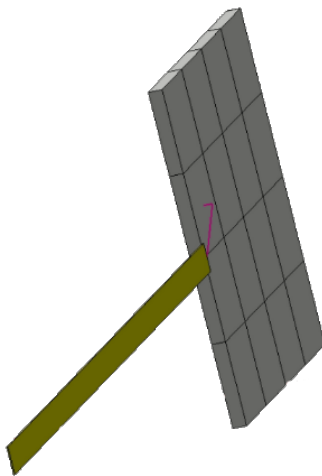


Figure 5.31: Antenna connected to a lateral board through a UDC in ESATAN.

References

- [1] UPC NanoSat Lab. IEEE Open PocketQube Kit Wiki. <https://wiki.nanosatlab.space/>, 2024.